AN ALIGNMENT-BY-RECONSTRUCTION ALGORITHM

João Sanches Jorge S. Marques

Instituto Superior Técnico, Instituto de Sistemas e Robótica
Lisbon, Portugal

ABSTRACT

In this paper we propose a reconstruction algorithm with alignment for free-hand 3D ultrasound. A set of ultrasound images with the associated positions and orientations are stored and used to reconstruct a given region of interest (ROI). In freehand ultrasound, the inspection planes are not parallel nor uniformly spaced. The proposed reconstruction algorithm deals with this non uniform sampling of the ROI and with the misalignment that arises due the position measurement errors and due the natural displacement of the organs during the medical exam. The acquired images are aligned w.r.t. the reconstructed volume in a iterative process, based on the optimization of a common energy function[1].

1. INTRODUCTION

This paper describes an algorithm for volume reconstruction from a set of ultrasound images corresponding to non parallel cross-sections of the human body[2]. The images are obtained with a free-hand ultrasound acquisition system[3]. This acquisition system uses an electromagnetic spatial locator attached to the ultrasound probe, providing real time measurements of the position and orientation of the probe. This allows the computation of the 3D position of the image pixels. The probe is manipulated by the medical doctor in a free way.

The anatomy estimation in this context, presents three main difficulties; i) speckle noise corrupting the ultrasound images, ii) non uniform sampling of the volume of interest (VOI) and iii) misalignment of the images due measurement errors or organ displacements. Therefore, the reconstruction algorithm must perform the following tasks: i) noise reduction, ii) interpolation and iii) alignment. These three tasks are often performed in three different steps of the reconstruction algorithm [3, 4, 5, 6].

In this paper we propose an algorithm, called *alignment-by-reconstruction*, where the three different tasks are performed simultaneously in a Bayesian framework with the MAP criterion [7]. An energy function is derived, based on the posteriori density function, depending on the observations, volume coefficients and alignment parameters [8]. The reconstruction is obtained by iteratively minimizing this energy w.r.t. the volume to be estimated and alignment parameters. Each iteration estimates new and improved versions of the volume and the alignment parameters. These two steps alternates until convergence is achieved. We stress that both steps optimize the same energy function instead of different adjustment criteria as it happens in many works.

The structure of the paper is the following: section 2 describes the experimental setup and formulates mathematically the reconstruction algorithm. Section 3 describes the solution of the problem formulated in 2 and in section 4 we present two application examples using synthetic and real data. Section 5 concludes the paper.

2. PROBLEM FORMULATION

Let us consider a scalar function describing the acoustic properties of the volume of interest (VOI), i.e., $f : \Omega \rightarrow R$ where $\Omega \in \mathbb{R}^3$ is the VOI. The function $f(x)$is given by

$$f(x) = \Phi(x)^T F \tag{1}$$

where $\Phi(x) = \{\phi_1(x), \phi_2(x), ..., \phi_N(x)\}^T$ is a N dimensional vector of basis functions and $F = \{f_1, f_2, ..., f_N\}$ is a set of coefficients to be estimated [9, 8]. The basis functions are locally supported and are located at the nodes of a 3D regular grid as shown in fig. 1.

The reconstruction problem is the following: given a set of observations $Y = \{y_i, y_2, ..., y_M\}$, and the correspondent locations $X = \{x_1, x_2, ..., x_M\}$ estimate the coefficients F that define the function $f(x)$. Each observation y_i corresponds to a pixel of an observed cross section of the VOI. This problem is solved in a Bayesian framework using the MAP criterion. The reconstruction algorithm must deal with i) speckle noise that corrupts the ultrasound images (noise reduction), ii) lack of data and multiple observations resulting from the non uniform sampling of the VOI (interpolation) and iii) position measurement errors and organ displacements (alignment).

Corresponding author: J. Sanches (jmrs@alfa.ist.utl.pt)

[1]The work presented in this paper was published in [1]

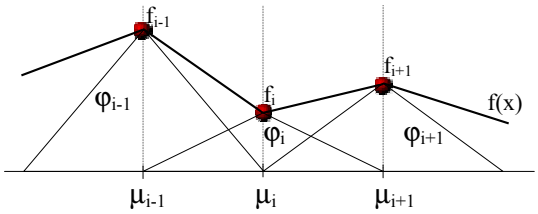

(a) Linear combination of finite supported basis functions (1D).

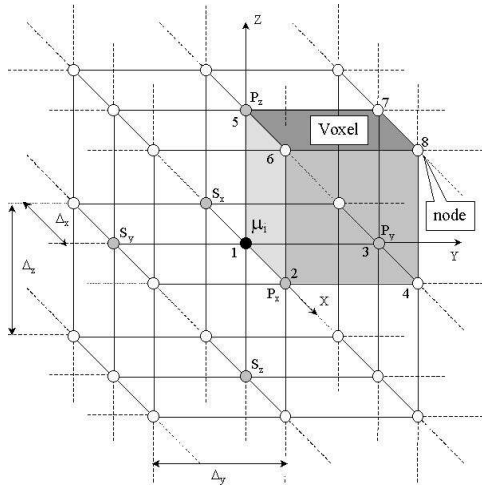

(b) 3D regular grid.

Fig. 1. Discrete representation of the function $f(x)$.

The function $f(x)$ can be obtained by jointly minimizing an energy function w.r.t. F and T, i.e.,

$$[\hat{F}, \hat{T}] = \arg\min_{F,T} E(F, T) \tag{2}$$

where F is the set of coefficients defining the function to be estimated, $f(x)$, T is the set of alignment parameters and

$$E(F, T) = -\log(p(Y|F, T)) - \log(p(F)) - \log(p(T)). \tag{3}$$

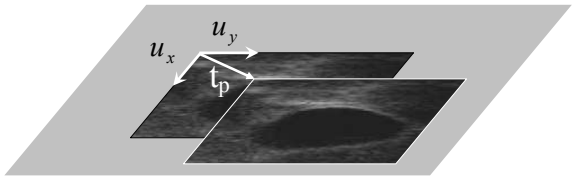

Fig. 2. Alignment vector for pth cross-section.

1. $p(Y|F, T)$ is the data fidelity term accounting for the speckle noise. Assuming statistical independency of the observations [11] and a Rayleigh distribution for the pixel intensities [10], the data fidelity term is

$$\log(p(Y|F, T)) = \sum_{i=1}^{M} \left[\log\left(\frac{y_i}{f(x_i + t_i)} \right) - \frac{y_i^2}{2f(x_i + t_i)} \right] \tag{4}$$

where t_i is a displacement vector associated to ith pixel y_i.In fact we will assume that all the displacement vectors associated to the same image are equal. Therefore t_i can be replaced by t_p were p is the image index.

2. $p(F)$ is the prior associated to the vector F to be estimated and it plays an important role when there is lack of data since it allows the estimation of non-observed regions from the observed ones by interpolation. In this paper we assume that f is smooth and $p(F)$ is a Gibbs distribution with quadratic potential functions [12], i.e.,

$$p(F) = \frac{1}{Z} e^{-\alpha U(F)} \tag{5}$$

where α is the regularization parameter and $U(F) = \sum_{(p,q)\in S} \delta_{pq}^2$ is the internal energy with $\delta_{pq}^2 = (f_p - f_q)^2$. This energy is obtained by summing all square differences among neighbouring nodes in the neighborhood system S.

3. $p(T)$ is the distribution of the error displacement vectors associated to the cross-sections, $T = \{t_1, ..., t_M\}$. It is assumed that each displacement vector, $t_p = d_x^p u_x^p + d_y^p u_y^p$, belongs to the inspection plane with u_x^p and u_y^p being vectors pointing along the two main directions of the pth cross-section, as shown in Fig.2. The coefficients d_τ^p are considered independent and normally distributed, $d^p = [d_x^p, d_y^p]^T \sim \mathcal{N}(0, \sigma^2 I)$ and therefore,

$$p(T) = p(D) = C \prod_{k=1}^{L} e^{-\frac{(d_x^k)^2 + d_y^k)^2}{2\sigma^2}} \tag{6}$$

where L is the number of cross-sections and $D = [d^1, d^2, ..., d^L]$.

3. RECONSTRUCTION

The solution of (2) is obtained by finding the stationary point of $E(F, D)$ w.r.t. F and D, i.e., $\nabla_{F,D} E(F, D) = 0$. This is performed iteratively in two main steps,

$$\nabla_F E(F, \hat{D}_{t-1}) = 0 \rightarrow \hat{F}_t \tag{7}$$

$$\nabla_D E(D, \hat{F}_t) = 0 \rightarrow \hat{D}_t \tag{8}$$

where t denotes the tth iteration. These two steps alternates until convergence is achieved.

Thus, the energy function is

$$E(F,D) = \sum_{i=1}^{N}\left[\frac{y_i^2}{2f(\hat{x}_i)} - \log\left(\frac{y_i}{f(\hat{x}_i)}\right)\right] + \frac{1}{2\sigma^2}\sum_{k=1}^{L}(d_x^p)^2 + (d_y^p)^2 + \alpha\sum_{(p,q)\in S}(f_p - f_q)^2. \quad (9)$$

where $f(x) = \sum_{k=1}^{N} f_k\phi_k(x)$ and $\hat{x_i} = x_i + t_p$. To solve the equations (7-8) we will use the Gauss-Seidel and fixed point methods by optimizing the energy function w.r.t. each parameter, f_i or d_τ^p at a time, dealing with all other unknowns as constants [13].

Thus

$$\frac{\partial E(F,D)}{\partial f_k} = 0 \Rightarrow \hat{f}_k^{t+1} = \frac{1}{4\alpha N_v}\sum_{i=1}^{M}\theta_i\phi_k(\hat{x}_i) + \bar{f}_k^t \quad (10)$$

$$\frac{\partial E(F,D)}{\partial d_\tau^p} = 0 \Rightarrow (d_\tau^p)^{t+1} = \frac{\sigma^2}{2}\sum_{i\in I_p}\theta_i(\underbrace{\nabla f(\hat{x}_i).u_\tau^p}_{\text{dot product}}) \quad (11)$$

where $\theta_i = \frac{y_i^2 - 2f^t(\hat{x}_i)}{(f^t(\hat{x}_i))^2}$, N_v is the number of neighbors of f_k (in this case $N_v = 6$) and $\bar{f}_k^t = (1/N_v)\sum_{(p\in V_k)}\hat{f}_p^t$ is the average intensity in the neighborhood of f_k. In the computation of the alignment parameters, d_τ^p, only the pixels belonging to the pth cross-section are used.

The initialization of the unknowns is performed as follows,

$$f_k^0 = \tilde{f}_k^{ML} \qquad d_\tau^p = 0$$

where $\tilde{f}_k^{ML}$ is an approximation of the maximum likelihood estimates given by

$$\tilde{f}_k^{ML} = \frac{1}{2}\frac{\sum_{i\in V(f_k)} y_i^2\phi_k(x_i)}{\sum_{i\in V(f_k)}\phi_k(x_i)} \quad (12)$$

where it was assumed that $f(x_i) \approx f_k$ when x_i is in the neighborhood of f_k, $V(f_k)$.

Fig.3 shows the reconstruction results for two different iterations using synthetic data. Fig.3.a) shows an original noisy image and Figs.3.b-c) show the corresponding cross-sections extracted from the reconstruction results at the end of iterations 1 and 8, respectively. Fig.3.d-e) displays the energy function w.r.t the two alignment parameters for this specific image in the first and 8th iterations respectively. As shown, this energy surface becomes sharper along the iterative process, which means that in the first iterations only a coarse alignment is performed and as reconstruction improves the alignment process also becomes more accurate.

.

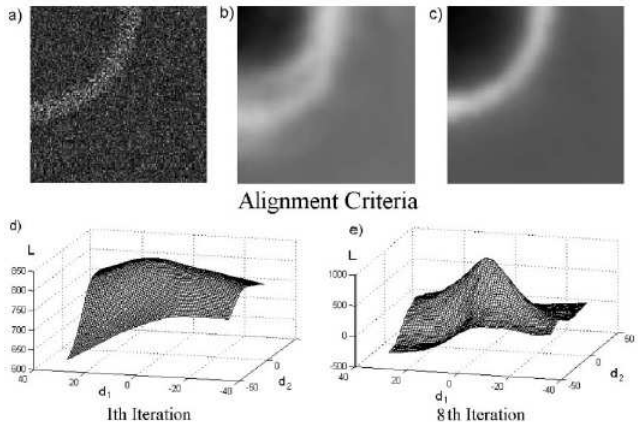

Fig. 3. a)Noisy image and reconstruction results with alignment in the b) first iteration and in the c) 8th iteration. The second line displays the energy function w.r.t the two alignment parameters in the d) first and e) 8th iterations respectively

4. EXPERIMENTAL RESULTS

In this section two examples are presented with synthetic and real data. The synthetic data is formed by a set of 50 images corrupted with white Rayleigh noise. These images corresponds to co-planar cross-section of a cylinder with radius r as shown in Fig.4. The coordinates of the image center are modified by a random displacement with normal distribution $\mathcal{N}(0,\sigma^2)$. The reconstruction was performed for several values of σ^2 and for each value 20 experiments were done. The bias and standard deviation of the alignment errors were computed. Notice that in this case we know the real position of each cross-section, allowing to compute the final alignment error. The standard deviation of the alignment error is displayed in Fig.5. It is concluded from these experiments that the displacement estimates are unbiased and accurate alignment is achieved for $\sigma < 0.8r$.

In the experiments with real data, a set of 64 non parallel cross-sections of a gall bladder is used. Figs.6 displays a set of 3 noisy cross-sections (a) and the corresponding cross-sections extracted from the reconstructed volumes in two cases; (b) without and (c) with alignment compensation. Fig.7 displays two new cross sections, embracing the whole VOI, extracted from both reconstructed volumes obtained a) without and b) with alignment. This figure shows the presence of artifacts resulting from the misalignment of the images. As observed in the third line of Fig.6, these artifacts almost disappear when the alignment compensation is included in the reconstruction algorithm.

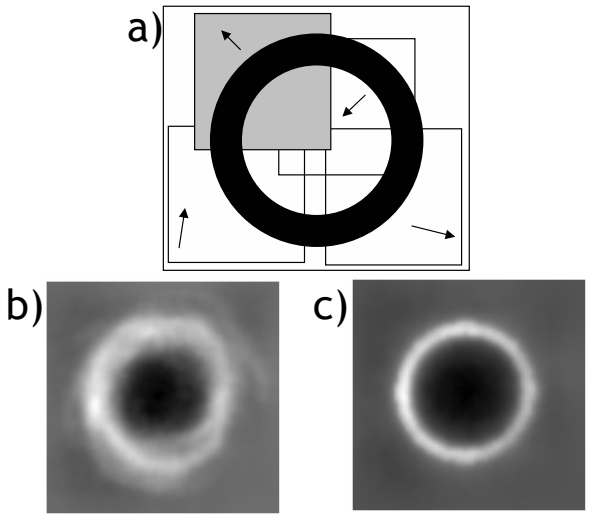

Fig. 4. Synthetic data. a) Co-planar cross-sections with intensity Rayleigh noise and Gaussian position noise. A new cross-section containing the original object is extracted from the reconstructed volumes/images b)without and c) with alignment.

5. CONCLUSION

In this paper we presented a reconstruction algorithm for 3D ultrasound based on a free-hand ultrasound acquisition setup. The proposed reconstruction algorithm deals simultaneously with noise reduction (denoising), non uniform sampling and lack of data (interpolation) and misalignments errors due position measurement errors and organ displacements.

The reconstruction algorithm is formulated in a Bayesian framework, using the MAP criterion. This problem is solved by minimizing an energy function w.r.t. the function to be estimated an w.r.t. the alignment parameters. These two steps alternates during the iterative algorithm until convergence is achieved, i.e., the function describing the anatomy in the VOI is simultaneously estimated with the alignment parameters needed to compensate for the position measurement errors and organ displacements.

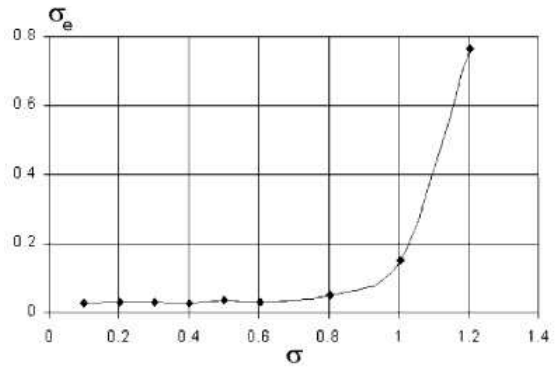

Fig. 5. Standard deviation of the alignment error, σ_e, as function of the standard deviation of the misalignment error σ, normalized by the radius r.

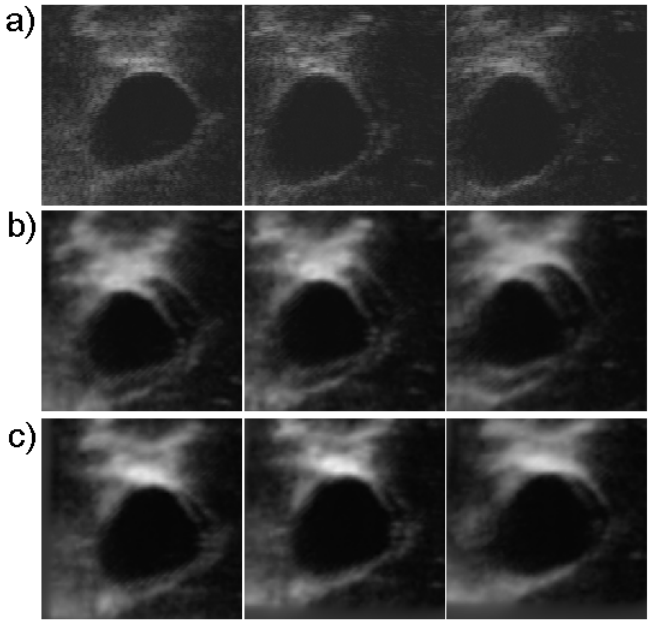

Fig. 6. Real data formed formed by 64 non-parallel cross-sections of a gall bladder.

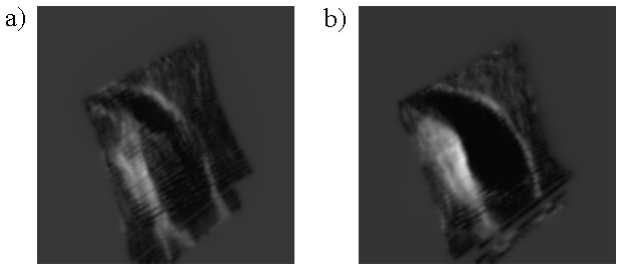

Fig. 7. New cross-section extracted from the reconstructed volumes a)not using and b)using the alignment algorithm.

Experimental results with synthetic and real data are used to illustrate the application of the alignment by reconstruction algorithm. In the case of synthetic data, montecarlo tests were performed to evaluate the capacity of the alignment algorithm to compensate for different levels of misalignment errors.

It is conclude, in both cases, that alignment plays a key role to obtain an accurate reconstruction of the volume of interest.

6. REFERENCES

[1] Sanches J., and Marques J.S., Joint Image Registration and Volume Reconstruction for 3D Ultrasound, Special Issue on 3D Ultrasound, Pattern Recognition Letters 24(2003) 791-800.

[2] J. Quistgaard, Signal Acquisition and Processing in Medical Diagnostics Ultrasound, IEEE Signal Processing Magazine, vol.14, no.1, pp. 67-74, January 1997.

[3] T.Nelson, D.Downey, D.Pretorius, A.Fenster,Three-Dimensional Ultrasound, Lippincott, 1999.

[4] R.N.Rohling, A. H. Gee and L. Berman, A comparation of freehand three-dimensional ultrasound reconstruction techniques, Medical Image Analysis, vol.4, no.4, pp.339-359, 1999.

[5] S. Ogawa and al., Three Dimension Ultrasonic Imaging for Diagnosis of Beast Tumor, Proc. British Machine Vision Conference, Edinburgh, pp.1677-1680, 1998.

[6] T.R.Nelson, D.H.Pretorius, Interactive Acquisition, Analysis and Visualization of Sonographic Volume Data, International Journal of Imaging Systems and Technology, vol.8, pp.26-37, 1997.

[7] S. Alliney. An algorithm for the minimization of mixed l and l norms with application to bayesian estimation. IEEE Signal Processing, 42(3):618-627, 1994.

[8] J. Sanches, J.Marques, A Rayleigh reconstruction/interpolation algorithm for 3D ultrasound, Pattern Recognition Letters, 21, pp. 917-926, 2000.

[9] Rohling R., Gee A., Berman L.,Treece G., Radial basis function interpolation for 3D freehand ultrasound. Proc. of the 16th ICIPMI, pp.478-483, Visegrad, Hungary, June 1999.

[10] C.Burckhardt, Speckle in Ultrasound B-Mode Scans, IEEE Trans. on Sonics and Ultrsonics, vol. SU-25, no.1, pp. 1-6, January 1978.

[11] E. Rignot, R. Chelappa, Segmentation of polarimetric sunthetic aperture radar data, IEEE Trans. Image Processing, vol.1, no.1, pp. 281-300, 1992.

[12] S. Geman and D. Geman, Stochastic Relaxation, Gibbs Distributions, and the Bayesian Restoration of Images, IEEE Trans on Pattern Analysis and Machine Intelligence, vol.PAMI-6, no.6, pp.721-741, November 1984.

[13] W.H.Press, W.T.Vetterling, S.A.Teukolsky and B.P.Flanner, Numerical Recipes in C, Cambridge University Press, 1994